

## ORIGINAL ARTICLE

# Growth, CO<sub>2</sub> consumption and H<sub>2</sub> production of *Anabaena variabilis* ATCC 29413-U under different irradiances and CO<sub>2</sub> concentrations

H. Berberoğlu<sup>1</sup>, N. Barra<sup>1</sup>, L. Pilon<sup>1</sup> and J. Jay<sup>2</sup>

<sup>1</sup> Mechanical and Aerospace Engineering Department, Henry Samueli School of Engineering and Applied Science, University of California Los Angeles, Los Angeles, CA, USA

<sup>2</sup> Civil and Environmental Engineering Department, Henry Samueli School of Engineering and Applied Science, University of California Los Angeles, Los Angeles, CA, USA

## Keywords

xxxxx, xxxx.

## Correspondence

Laurent Pilon, Mechanical and Aerospace Engineering Department, Henry Samueli School of Engineering and Applied Science, University of California Los Angeles, Los Angeles, CA 90095, USA.  
E-mail: pilon@seas.ucla.edu

2007/0021: received 9 January 2007, revised 31 May 2007 and accepted 1 July 2007

doi:10.1111/j.1365-2672.2007.03559.x

## Abstract

**Aims:** The objective of this study is to develop kinetic models based on batch experiments describing the growth, CO<sub>2</sub> consumption, and H<sub>2</sub> production of *Anabaena variabilis* ATCC 29413-U<sup>TM</sup> as functions of irradiance and CO<sub>2</sub> concentration.

**Methods and Results:** A parametric experimental study is performed for irradiances from 1120 to 16100 lux and for initial CO<sub>2</sub> mole fractions from 0.03 to 0.20 in argon at pH 7.0 ± 0.4 with nitrate in the medium. Kinetic models are successfully developed based on the Monod model and on a novel scaling analysis employing the CO<sub>2</sub> consumption half-time as the time scale.

**Conclusions:** Monod models predict the growth, CO<sub>2</sub> consumption and O<sub>2</sub> production within 30%. Moreover, the CO<sub>2</sub> consumption half-time is an appropriate time scale for analysing all experimental data. In addition, the optimum initial CO<sub>2</sub> mole fraction is 0.05 for maximum growth and CO<sub>2</sub> consumption rates. Finally, the saturation irradiance is determined to be 5170 lux for CO<sub>2</sub> consumption and growth whereas, the maximum H<sub>2</sub> production rate occurs around 10 000 lux.


**Significance and Impact of the Study:** The study presents kinetic models predicting the growth, CO<sub>2</sub> consumption and H<sub>2</sub> production of *A. variabilis*. The experimental and scaling analysis methods can be generalized to other microorganisms.

## Introduction

Increased amounts of greenhouse gas emissions as well as the exhaustion of easily accessible fossil fuel resources are calling for effective CO<sub>2</sub> mitigation technologies and clean and renewable energy sources. Hydrogen, for use in fuel cells, is considered to be an attractive alternative fuel since water vapour is the only byproduct from its reaction with oxygen. Hydrogen production by cultivation of cyanobacteria in photobioreactors offers a clean and renewable alternative to thermochemical or electrolytic hydrogen production technologies with the added advantage of CO<sub>2</sub> mitigation. In particular, *Anabaena variabilis*

is a cyanobacterium capable of mitigating CO<sub>2</sub> and producing H<sub>2</sub>. The objective of this study is to investigate experimentally the CO<sub>2</sub> mitigation, growth, and H<sub>2</sub> production of *A. variabilis* ATCC 29413-U<sup>TM</sup> in BG-11 medium under atmosphere containing argon and CO<sub>2</sub>. Parameters investigated are the irradiance and the initial CO<sub>2</sub> mole fraction in the gas phase.

The cyanobacterium *A. variabilis* is a photosynthetic prokaryote listed among the potential candidates for hydrogen production (Pinto *et al.* 2002), whose genome sequence has been completed (of Energy 2007). Moreover, *A. variabilis* and its mutants are of great interest in research as hydrogen producers (Hansel and Lindblad

	J	A	M	3	5	5	9	B	Dispatch: 5.9.07	Journal: JAM	CE: Ulagammal
	Journal Name			Manuscript No.					Author Received:	No. of pages: 16	PE: Raymond

1998; Tsygankov *et al.* 1998; Borodin *et al.* 2000; Happe *et al.* 2000; Pinto *et al.* 2002; Yoon *et al.* 2002). *Anabaena variabilis* utilizes light energy in the spectral range from 400 to 700 nm, known as photosynthetically active radiation (PAR), and consumes CO<sub>2</sub> to produce biomass, oxygen and hydrogen. The reader is referred to Refs. (Benemann 2000; Madamwar *et al.* 2000; Das and Veziroglu 2001; Pinto *et al.* 2002; Prince and Ksheshgi 2005) for detailed reviews of photobiological hydrogen production. In brief, *A. variabilis* utilizes water as its electron donor (Prince and Ksheshgi 2005) and produces hydrogen mainly using nitrogenase enzyme (Madamwar *et al.*, 2002). The primary role of nitrogenase is to reduce nitrogen to ammonia during nitrogen fixation (Das and Veziroglu 2001). H<sub>2</sub> is produced as a by product of this reaction (Das and Veziroglu 2001). In the absence of molecular nitrogen, nitrogenase will reduce protons and catalyze the production of H<sub>2</sub> provided reductants and ATP are present (Das and Veziroglu 2001). Nitrogenase enzyme is located in special cells called heterocysts, which protect nitrogenase from O<sub>2</sub> inhibition (Tsygankov *et al.* 1998). However, at dissolved O<sub>2</sub> concentrations higher than 50 µmol l<sup>-1</sup>, the produced H<sub>2</sub> is consumed by *A. variabilis* in a reaction catalyzed by the enzyme 'uptake' hydrogenase (Tsygankov *et al.* 1998), thus reducing the net H<sub>2</sub> production rate (Tsygankov *et al.* 1998). Finally, *A. variabilis* also possesses bi-directional hydrogenases located at the cytoplasmic membrane (Madamwar *et al.* 2000). However, unlike nitrogenase, these enzymes are not well protected from oxygen and their functioning is inhibited at relatively low O<sub>2</sub> concentrations (Benemann 2000).

Table 1 summarizes previous studies on H<sub>2</sub> production by *A. variabilis*. It indicates the strain used, the gas phase composition, irradiance and the medium used during growth and H<sub>2</sub> production stages, as well as the specific growth, CO<sub>2</sub> consumption, and H<sub>2</sub> production rates. Briefly, Tsygankov *et al.* (1998) and Sveshnikov *et al.* (1997) studied the hydrogen production by *A. variabilis* ATCC 29413 and by its mutant PK84, lacking the hydrogen uptake metabolism. On the other hand, Markav *et al.* (1993) proposed a two stage photobioreactor alternating between (i) growth and (ii) H<sub>2</sub> production phases for attaining high H<sub>2</sub> production rates. During the growth phase cyanobacteria fix CO<sub>2</sub> and nitrogen from the atmosphere to grow and produce photosynthates. In the H<sub>2</sub> production phase, they utilize the photosynthates to produce H<sub>2</sub>. In addition, Yoon *et al.* (2002) used a two stage batch process and suggested an improvement on the first stage by incorporating nitrate in the growth medium for faster growth of *A. variabilis*. As opposed to using a two stage photobioreactor, Markov *et al.* (1997b) demonstrated a single stage photobioreactor using *A. variabilis*

PK-84 in a helical photobioreactor. More recently, Tsygankov *et al.* (2002) demonstrated a single stage photobioreactor operation for H<sub>2</sub> production using *A. variabilis* PK-84 in an outdoor photobioreactor similar to that of Markov *et al.* (1997b).

Most previous studies using *A. variabilis* have used a two stage photobioreactor with relatively limited ranges of CO<sub>2</sub> concentrations and light irradiance. In addition, to the best of our knowledge, there has been no reported study simultaneously varying irradiance and the initial CO<sub>2</sub> mole fraction in the gas phase to assess quantitatively the CO<sub>2</sub> mitigation, growth, and H<sub>2</sub> production of *A. variabilis* in a single stage process. The objectives of this work are (i) to develop kinetic models based on batch experiments describing the growth, CO<sub>2</sub> consumption and H<sub>2</sub> production of *A. variabilis* ATCC 29413-U<sup>TM</sup> as functions of irradiance and CO<sub>2</sub> concentration and (ii) to provide recommendations on the optimum irradiance and the gas phase CO<sub>2</sub> mole fraction for achieving rapid growth, high CO<sub>2</sub> uptake and H<sub>2</sub> production rates.

## Materials and methods

A cyanobacterial suspension was prepared from a 7-day-old culture. The micro-organism concentration denoted by  $X$  was adjusted to 0.02 kg dry cell m<sup>-3</sup> by diluting the culture with fresh medium and was confirmed by monitoring the optical density (OD). Then, 60 ml of the prepared suspension was dispensed in 160-ml serum vials. The vials were sealed with butyl rubber septa, crimped and flushed through the septa with industrial grade argon, sterilized with 0.2 µm pore size syringe filter, for 10 min with a needle submerged in the liquid phase. The initial CO<sub>2</sub> mole fraction in the head-space, denoted by  $x_{\text{CO}_2, \text{g}, 0}$ , was set at 0.03, 0.04, 0.08, 0.15 and 0.20. This was achieved first by adjusting the gauge pressure in the vials to -7.09, -10.13, -20.27, -30.40 and -40.53 kPa respectively. Then, 7, 10, 20, 30 and 40 ml of industrial grade CO<sub>2</sub> were injected into the vials, respectively, through a 0.2 µm pore size syringe filter. The vials were shaken until the head-space pressure stabilized indicating that both the partitioning of CO<sub>2</sub> between the gas and liquid phases and the dissolution of CO<sub>2</sub> in water were at equilibrium. Finally, the head-space was sampled to measure the initial CO<sub>2</sub> mole fraction. Each vial was prepared in duplicates. The vials were placed horizontally on an orbital shaker (model ZD-9556 by Madell Technology Group, USA) and stirred continuously at 115 rev min<sup>-1</sup> throughout the duration of the experiments. Continuous illumination was provided from the top of the orbital shaker. The transparent glass vials could be approximated to a cylindrical tube of diameter 50 mm, of height 80 mm, and of wall thickness 2 mm.

**Table 1** Summary of experimental conditions used and associated maximum specific growth, CO<sub>2</sub> consumption and H<sub>2</sub> production rates reported in the literature using various strains of *Anabaena variabilis*

<i>A. variabilis</i> strain	Stage I			Stage II			Maximum reported rates			
	Gas phase	Medium	Irradiance (lux)	Gas phase	Medium	Irradiance (lux)	$\mu$	$\psi_{\text{CO}_2}$	$\pi_{\text{H}_2}$	References
Kutzing 1403/4B	95 vol. % Air + 5 vol. % CO <sub>2</sub>	Allen and Arnon w/o nitrate at 25°C	1800	300 mm Hg vacuum	Same as stage I	13 000	N/A	7000	830	(Markov et al. 1995)
ATCC 29413	89 vol. % air + 11 vol. % CO <sub>2</sub>	BG-11 <sub>o</sub> + 3.5 mmol l <sup>-1</sup> NaNO <sub>3</sub> at 30°C	2500–5500	Argon	BG-11 <sub>o</sub> w/o nitrate at 30°C	9000–12 000	0.05	2700	80	(Yoon et al. 2002)
ATCC 29413	98 vol. % air + 2 vol. % CO <sub>2</sub>	Allen and Arnon w/o nitrate molybdenum replaced w/vanadium at 30°C	8000	Argon	Same as stage I	10 000–14 000	N/A	N/A	630	(Tsygankov et al. 1998)
PK 84	98 vol. % air + 2 vol. % CO <sub>2</sub>	Allen and Arnon w/o nitrate molybdenum replaced w/vanadium at 30°C	8000	Argon	Same as stage I	10 000–14 000	N/A	N/A	515	(Tsygankov et al. 1998)
ATCC 29413	73 vol. % Ar + 25 vol. % N <sub>2</sub> + 2 vol. % CO <sub>2</sub>	Allen and Arnon w/o nitrate molybdenum replaced w/vanadium at 30°C	6500	93 vol. % Ar + 5 vol. % N <sub>2</sub> + 2 vol. % CO <sub>2</sub>	Same as stage I	6500	N/A	N/A	720-37	(Sveshnikov et al. 1997)
PK 84	73 vol. % Ar + 25 vol. % N <sub>2</sub> + 2 vol. % CO <sub>2</sub>	Allen and Arnon w/o nitrate molybdenum replaced w/vanadium at 30°C	6500	93 vol. % Ar + 5 vol. % N <sub>2</sub> + 2 vol. % CO <sub>2</sub>	Same as stage I	6500	N/A	N/A	2600	(Sveshnikov et al. 1997)
PK 84	98 vol. % air + 2 vol. % CO <sub>2</sub>	Allen and Arnon w/o nitrate molybdenum replaced w/vanadium at 30°C	outdoor	98 vol. % Air + 2 vol. % CO <sub>2</sub>	Same as stage I	Outdoor	0.03	N/A	300	(Tsygankov et al. 2002)

The illuminated surface area of each vial was  $40 \times 10^{-4} \text{ m}^2$ . The irradiance, defined as the total radiant flux of visible light from 400 to 700 nm incident on a vial from the hemisphere above it, ranged from 1120 to 16 100 lux. Note that for the lamps used in the experiments 1 lux of irradiance was equivalent to  $3 \times 10^{-3} \text{ W m}^{-2}$  and  $14 \times 10^{-3} \mu\text{mol m}^{-2} \text{ s}^{-1}$  in the PAR.

Throughout the experiments CO<sub>2</sub>, H<sub>2</sub> and O<sub>2</sub> concentrations in the head-space as well as the cyanobacteria concentration and pH in the liquid phase were continually monitored. In addition, the temperature and pressure of the vials were measured to convert the molar fractions of gas species into volumetric mass concentrations. The irradiance incident on individual vials was recorded. Details of the experimental setup and procedures are given in the following sections.

### Cyanobacteria culture and concentration measurements

*Anabaena variabilis* ATCC 29413-U<sup>TM</sup> was purchased from the American Type Culture Collection (ATCC) and received in freeze dried form. The culture was activated with 10 ml of sterilized milli-Q water. It was cultivated and transferred weekly in ATCC medium 616 with air-CO<sub>2</sub> mixture in the head-space with an initial mole fraction of CO<sub>2</sub> of 0.05. One litre of ATCC medium 616 contained 1.5 g NaNO<sub>3</sub>, 0.04 g K<sub>2</sub>HPO<sub>4</sub>, 0.075 g MgSO<sub>4</sub>·7H<sub>2</sub>O, 0.036 g CaCl<sub>2</sub>·2H<sub>2</sub>O, 6.0 mg citric acid, 6.0 mg ferric ammonium citrate, 0.02 g Na<sub>2</sub>CO<sub>3</sub>, 1.0 mg EDTA and 1.0 ml of trace metal mix A5. One litre of trace metal mix A5 contains 2.86 g H<sub>3</sub>BO<sub>3</sub>, 1.81 g MnCl<sub>2</sub>·4H<sub>2</sub>O, 0.222 g ZnSO<sub>4</sub>·7H<sub>2</sub>O, 0.39 g Na<sub>2</sub>MoO<sub>4</sub>·2H<sub>2</sub>O, 0.079 g CuSO<sub>4</sub>·5H<sub>2</sub>O, 49.4 mg Co(NO<sub>3</sub>)<sub>3</sub>·6H<sub>2</sub>O. The pH of the medium was adjusted to be 7.3 by adding 1 mol l<sup>-1</sup> HCl and/or 1 mol l<sup>-1</sup> NaOH. Then, 20 ml of HEPES buffer solution at pH 7.3 was added to one litre of medium. Finally, the medium was autoclaved at 121°C for 40 min.

The cyanobacteria concentration *X* was determined by sampling 1 ml of bacteria suspension from the vials and measuring the OD. A calibration curve was created by measuring both the dry cell weight of a cyanobacteria suspension and the corresponding OD. First, the OD of the cyanobacteria was measured in disposable polystyrene cuvettes with light path of 10 mm at 683 nm (Yoon *et al.* 2002) using a UV-Vis spectrophotometer (Cary-3E; Varian, USA). Then, the bacteria suspension was filtered through mixed cellulose filter membranes with 0.45 μm pore size (HAWP-04700; Millipore, USA) and dried at 85°C over night. The dried filters were weighed immediately after being taken out of the oven on a precision balance (model AT261; Delta Range Factory, USA) with a precision of 0.01 mg. The calibration curve for OD was

generated by using 14 different bacteria concentrations ranging from 0.04 to 0.32 kg dry cell m<sup>-3</sup>. The relation between OD and bacteria concentration is linear for the OD range from 0 to 1.2 and 1 unit of OD corresponds to 0.274 kg dry cell m<sup>3</sup>.

### Temperature, pressure and pH

The temperature of the vials was measured with a thermocouple (Dual Thermometer; Fisher Scientific, USA). The heat from the high intensity fluorescent bulbs was removed by convective cooling using a fan to maintain a steady-state temperature of  $24 \pm 1^\circ\text{C}$  throughout the duration of the experiments. The head-space pressure was monitored with a digital gauge pressure sensor (model PX26-005GV; Omega Heater Company, USA) connected to a digital meter (model DP25B-S by Omega Heater Company). Finally, the pH of the medium was measured with a digital pH probe (model Basic AB Plus; Fisher Scientific).

### Lighting and light analysis

The irradiance incident on the vials  $G_{\text{in}}$  was provided by fluorescent light bulbs (Ecologic by Sylvania, USA and Fluorex by Lights of America, USA) and varied by changing the number of bulbs. The spectral irradiance of these bulbs were measured with a spectrophotometer (model USB2000, Ocean Optics) connected to a cosine collector over the spectral range from 350 to 750 nm. The spectral irradiance of the light bulbs  $G_{\lambda}$ , normalized with its maximum value  $G_{\text{max}}$  at 540 nm, along with the reported cyanobacterial absorption coefficient  $\kappa_{\lambda}$  (Merzlyak and Naqvi 2000), normalized with its maximum value  $\kappa_{\text{max}}$ , are presented in Fig. 1. The irradiance incident on the vials was measured with both a light meter (Fisherbrand Tracable Meter by Fisher Scientific) and a quantum sensor (LI-COR, Model LI-190SL; LI-COR Inc., USA). The total irradiance on each vial was measured individually in the PAR, i.e. within the spectral range from 400 to 700 nm. Due to experimental difficulties in achieving the exact same irradiance for all vials, five different irradiance ranges were explored namely, 1120–1265l, 1680–2430, 3950–4600, 7000–8700 and 14 700–16 100 lux.

### Gas analysis

The gas analysis was carried out every 24 h by sampling 500 μl of head-space volume of the vials. The concentrations of CO<sub>2</sub>, H<sub>2</sub> and O<sub>2</sub> in the head-space were measured with a gas chromatographer (HP-5890; Hewlett Packard) equipped with a packed column (Carboxen-1000; Supelco, USA) and a thermal conductivity detector

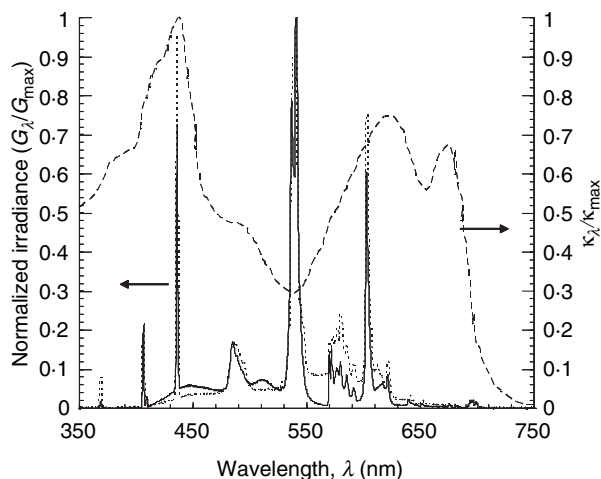


**Figure 1** The normalized spectral irradiance of Ecologic (solid line) and Fluorex (dotted line) light bulbs  $G_{\lambda}/G_{\max}$  along with the normalized absorption coefficient of *Anabaena variabilis* (dashed line)  $\kappa_{\lambda}/\kappa_{\max}$  (Merzlyak and Naqvi 2000).

(TCD). The gas chromatographer output was processed with an integrator (HP-3395, Hewlett Packard). Throughout the gas analysis, the injector and detector temperatures were maintained at 120°C. During the H<sub>2</sub> and O<sub>2</sub>, analysis argon was used as the carrier gas and the oven temperature was maintained at 35°C. The retention times for H<sub>2</sub> and O<sub>2</sub> were found to be 2.1 and 7.5 min respectively. On the other hand, during the CO<sub>2</sub> analysis, Helium was used as the carrier gas and the oven temperature was maintained at 255°C. The retention time for CO<sub>2</sub> was then 4.9 min. Calibration curves for the TCD

response were prepared at seven different known gas concentrations from  $16 \times 10^{-6}$  to  $3.2 \times 10^{-3}$  kg m<sup>3</sup> for H<sub>2</sub>, from  $25.6 \times 10^{-3}$  to  $1314 \times 10^{-3}$  kg m<sup>3</sup> for O<sub>2</sub> and from  $3.96 \times 10^{-3}$  to  $352 \times 10^{-3}$  kg m<sup>3</sup> for CO<sub>2</sub>. All calibration curves were linear within these gas concentration ranges. During the experiments, peak heights were recorded and correlated with the corresponding moles of gas using the respective calibration curves.

## Results

The experimental parameters used in the study along with the experimental labels are summarized in Table 2. In brief, the initial CO<sub>2</sub> mole fraction in the head-space,  $x_{\text{CO}_2, \text{g}, 0}$ , varied from 0.03 to 0.20 while the irradiance  $G$  varies from 1120 to 16 100 lux. Pressure, temperature and pH were maintained at  $1 \pm 0.1$  atm.,  $24 \pm 1$ °C and  $7.0 \pm 0.4$  respectively. To develop semi-empirical models for CO<sub>2</sub> consumption, growth, H<sub>2</sub> and O<sub>2</sub> production by *A. variabilis* ATCC 29413 using the experimental data, the following assumptions are made:

1. The concentration of gases in each phase and the concentration of cyanobacteria in the liquid phase are uniform within a given vial, due to vigorous mixing provided by the orbital shaker.
2. The Damkohler number, defined as the ratio of the reaction rate to the mass transfer rate (Smith *et al.* 1998), associated with the experimental setup is on the order of  $10^{-4}$ . Therefore, metabolic reactions of the cyanobacteria are not mass transfer limited (Smith *et al.* 1998).
3. The gas species in the liquid and gas phases are at quasi-equilibrium at all times.

**Table 2** Summary of the parameters used in the experiments

Label	G (lux)	$x_{\text{CO}_2, \text{g}, 0}$	$t_{1/2}$ (h)	$\mu_{\text{avg}}$ (1 h <sup>-1</sup> )	$Y_{X/\text{CO}_2}$ (kg kg <sup>-1</sup> )	$\psi_{\text{CO}_2}$ (kg kg <sup>-1</sup> h <sup>-1</sup> )
0GH	7000	0.20	74.4	0.024	0.373	0.065
0IJ	14700	0.20	65.3	0.028	0.352	0.081
1AB	1120	0.15	232.8	0.009	0.451	0.020
1CD	1680	0.15	189.3	0.013	0.589	0.023
1EF	3950	0.15	82.3	0.024	0.465	0.051
1GH	8700	0.15	49.5	0.033	0.398	0.082
1IJ	16100	0.15	46.8	0.036	0.381	0.094
2AB	1175	0.08	120.6	0.013	0.555	0.024
2CD	1820	0.08	98.4	0.016	0.626	0.026
2EF	4300	0.08	53.2	0.027	0.489	0.055
2GH	8000	0.08	37.1	0.038	0.440	0.086
2IJ	16100	0.08	39.1	0.041	0.433	0.094
3AB	1195	0.04	71.4	0.018	0.685	0.026
3CD	1815	0.04	57.3	0.022	0.755	0.030
3EF	4190	0.04	32.0	0.037	0.629	0.059
4AB	1265	0.03	64.9	0.017	0.840	0.020
4CD	2430	0.03	73.8	0.023	0.859	0.026
4EF	4600	0.03	27.3	0.029	0.748	0.038

4. *A. variabilis* both consumes and produces CO<sub>2</sub>, O<sub>2</sub> and H<sub>2</sub>. Therefore, the reported gas phase concentration of species correspond to the net consumed or produced quantities.

5. The only parameters affecting the bacterial growth and product formation are the CO<sub>2</sub> concentration and the irradiance  $G$ . The supply of other nutrients such as minerals and nitrate are assumed to be unlimited in the growth medium.

6. Given the pH range, the effect of buffer capacity on the growth rate is assumed to be negligible compared with the effects of CO<sub>2</sub> concentration and local irradiance.

7. The death of micro-organisms is neglected the time frame of the experiments.

### Kinetic modelling

During the growth phase, the time rate of change of micro-organism concentration  $X$  can be written as (Dunn *et al.* 2003),

$$\frac{dX}{dt} = \mu X, \quad (1)$$

where  $\mu$  is the specific growth rate of the cyanobacteria expressed in s<sup>-1</sup>. In this study, it is assumed to be a function of (i) the average available irradiance denoted by  $G_{av}$  and (ii) the concentration of total dissolved inorganic carbon within the cyanobacterial suspension denoted by  $C_{TOT}$ . The specific growth rate has been modelled using the Monod model taking into account (i) light saturation; (ii) CO<sub>2</sub> saturation; and (iii) CO<sub>2</sub> inhibition as (Asenjo and Merchuk 1995):

$$\mu = \mu_{max} \left( \frac{G_{av}}{G_{av} + K_G} \right) \left( \frac{C_{TOT}}{K_C + C_{TOT} + C_{TOT}^2/K_I} \right), \quad (2)$$

where  $\mu_{max}$  is the maximum specific growth rate,  $K_G$  is the half-saturation constant for light,  $K_C$  and  $K_I$  are the half-saturation and the inhibition constants for dissolved inorganic carbon respectively. First, the spectral and local irradiance  $G_\lambda(z)$  within the suspension is estimated using Beer–Lambert's law as:

$$G_\lambda(z) = G_{\lambda,in} \exp(-E_{ext,\lambda} X z), \quad (3)$$

where  $G_{\lambda,in}$  is the spectral irradiance incident on the vials,  $z$  is the distance from the top surface of the suspension,  $X$  is the micro-organism concentration in kg dry cell m<sup>-3</sup>,  $E_{ext,\lambda}$  is the spectral extinction cross-section of *A. variabilis* at wavelength  $\lambda$ . Note that  $E_{ext,\lambda}$  varies by <4% over the PAR and is assumed to be constant and equal to  $E_{ext,PAR} = 350 \text{ m}^2 \text{ kg}^{-1} \text{ dry cell}$  (Berberoğlu and Pilon 2007). Then, the available irradiance  $G_{av}$  can be estimated by averaging the local irradiance over the depth of the culture  $L$  as:

$$G_{av} = \frac{1}{L} \int_0^L G(z) dz \quad \text{where} \quad G(z) = G_{in} \exp(-E_{ext,PAR} X z), \quad (4)$$

Experimentally  $L$  is equal to 0.02 m.

Finally,  $C_{TOT}$  is the total dissolved inorganic carbon concentration in the liquid phase expressed in kmol m<sup>-3</sup>. It depends on the pH of the medium and on the molar fraction of CO<sub>2</sub> in the gas phase  $x_{CO_2,g}$  and can be written as (Benjamin 2002):

$$C_{TOT} = 10^{-1.5} x_{CO_2,g} + \left( \frac{10^{-7.8}}{10^{-pH}} \right) x_{CO_2,g} + \left( \frac{10^{-28.1}}{10^{-2pH}} \right) x_{CO_2,g}, \quad (5)$$

where the three terms on the right hand side correspond to H<sub>2</sub>CO<sub>3</sub><sup>\*</sup>, HCO<sub>3</sub><sup>-</sup>, and CO<sub>3</sub><sup>2-</sup> concentrations in the liquid phase respectively.

The values of the parameters  $\mu_{max}$ ,  $K_G$ ,  $K_C$ , and  $K_I$  in eqn (2) are estimated by minimizing the root mean square error between the experimentally measured cyanobacteria concentrations and the model predictions obtained by integrating eqns (1) and (2). The associated parameters along with those reported by Erickson *et al.* (1987) for the cyanobacteria *Spirulina platensis* are summarized in Table 3. Figure 2(a) compares the cyanobacteria concentrations measured experimentally with the model predictions. It indicates that the model predicts the experimental data for micro-organism concentration within 30%.

Moreover, assuming that the biomass yield based on consumed carbon and denoted by  $Y_{X/C}$  is constant, as assumed by Erickson *et al.* (1987), the total dissolved inorganic carbon concentration can be modelled as (Dunn *et al.* 2003):

$$\frac{dC_{TOT}}{dt} = -\frac{\mu}{Y_{X/C}} X, \quad (6)$$

The yield  $Y_{X/C}$  can be expressed in terms of the biomass yield based on consumed CO<sub>2</sub> denoted by  $Y_{X/CO_2}$  as  $Y_{X/C} = M_{CO_2} Y_{X/CO_2}$  where  $M_{CO_2}$  is the molecular weight of

**Table 3** Summary of the parameters used in kinetic modeling of *Anabaena variabilis*

Parameter	Present study	Erickson <i>et al.</i> (1987)	Equation
$\mu_{max}$ (1 h <sup>-1</sup> )	0.10	0.12	Eqn (2)
$K_G$ (lux)	4440	4351	Eqn (2)
$K_C$ (kmol C m <sup>-3</sup> )	0.0002	0.0002	Eqn (2)
$K_I$ (kmol C m <sup>-3</sup> )	0.0182	N/A	Eqn (2)
$Y_{X/C}$ (kg dry cell kmol <sup>-1</sup> C)	24.96	25.18	Eqn (6)
$Y_{O_2/X}$ (kg O <sub>2</sub> kg <sup>-1</sup> dry cell)	1.28	N/A	Eqn (7)

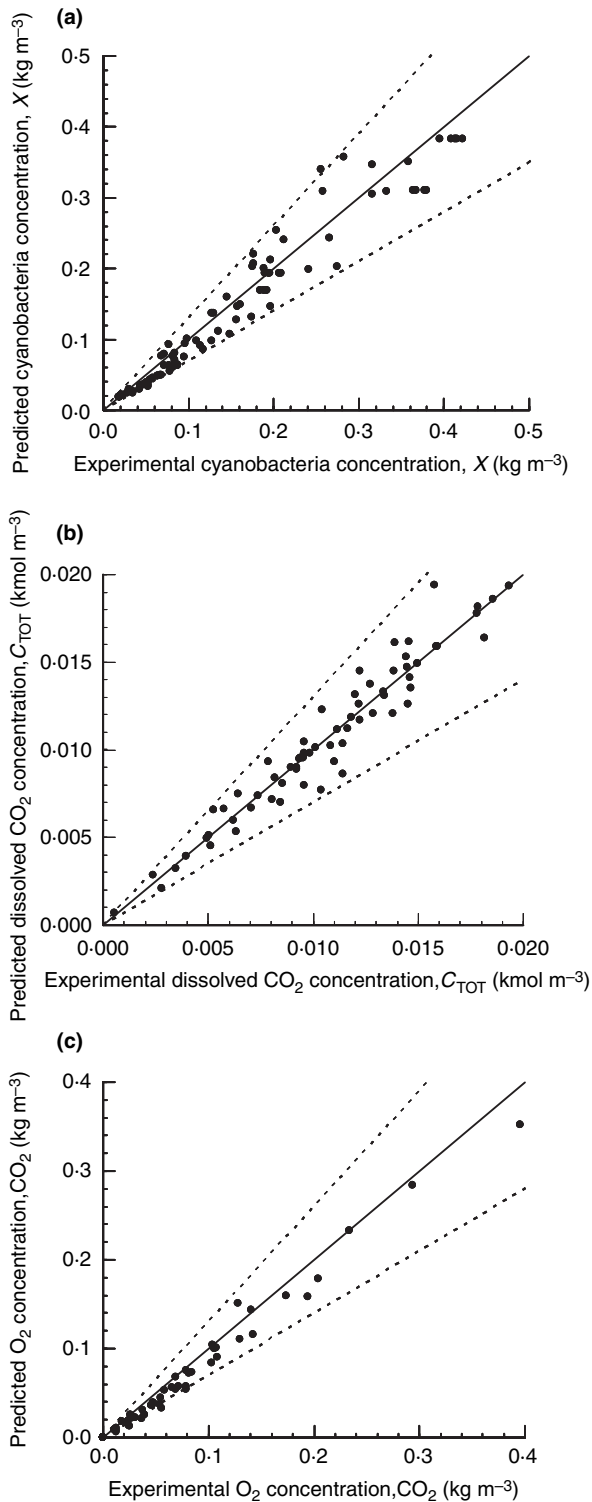


**Figure 2** Comparison between experimental data and kinetic model predictions for (a) cyanobacterial concentration [eqn (2)], (b) total dissolved inorganic carbon concentration [eqn (6)] and (c) total O<sub>2</sub> concentration [eqn (7)]. The dashed lines correspond to  $\pm 30\%$  deviation from model predictions.

CO<sub>2</sub> equal to 44 kg kmol<sup>-1</sup>. The value of  $Y_{X/CO_2}$  for each experiment is given in Table 2. The value of  $Y_{X/C}$  used in this study is the average value obtained across experiments which is equal to 24.96 kg dry cell kmol<sup>-1</sup> C. Figure 2(b) compares  $C_{TOT}$  obtained using eqn (5) and the measured pH and  $x_{CO_2,g}$  with the value predicted by integrating eqn (6). It shows that the model predicts the experimental data within 30%.

Furthermore, assuming that one mole of O<sub>2</sub> is evolved per mole of CO<sub>2</sub> consumed, the total oxygen concentration in the vial can be computed as,

$$\frac{dC_{O_2}}{dt} = Y_{O_2/X} \mu X, \quad (7)$$

where  $Y_{O_2/X}$  is the O<sub>2</sub> yield based on biomass and equal to 1.28 kg O<sub>2</sub> kg<sup>-1</sup> dry cell. It is expressed as  $M_{O_2}/Y_{X/C}$  where  $M_{O_2}$  is the molecular weight of O<sub>2</sub> equal to 32 kg kmol<sup>-1</sup>. Figure 2(c) compares the total O<sub>2</sub> concentration measured experimentally with that predicted by integrating eqn (7). It indicates that the experimental data for CO<sub>2</sub> falls within 30% of model's predictions.

Finally, models similar to eqns (6) and (7) were applied to the H<sub>2</sub> concentration in the headspace measured as a function of time. However, yield coefficients could not be obtained to model the experimental data within 30%.

### Scaling analysis

The models described in the previous section depend on quantities such as  $G_{av}$  and  $C_{TOT}$  that are not directly measurable. They are typically kept constant by using either a chemostat (Erickson *et al.* 1987) or a turbidostat (Goldman *et al.* 1974). However, construction and operation of these devices are relatively expensive and experimentally more challenging than the vial experiments performed in this study. Moreover, a number of assumptions had to be made to estimate the parameters of the kinetic models. Specifically,  $G_{av}$  was estimated using Beer-Lambert's law which does not take into account in-scattering by the micro-organisms and can lead to errors as high as 30% in estimating the local irradiance  $G_L(z)$  (Berberoğlu *et al.* 2007). Moreover, the growth rates of the micro-organisms were assumed to be independent of pH which varied between  $7.0 \pm 0.4$  during the course of the experiments. Furthermore, the average yields  $Y_{X/C}$  and  $Y_{O_2/X}$  were assumed to be constant in modeling the CO<sub>2</sub> consumption and O<sub>2</sub> production. Finally, modeling H<sub>2</sub> production with the approach above gave poor results. Therefore, as an alternative to the kinetic models described above, a novel scaling analysis is presented for analysing the data based on the directly measurable molar fraction  $x_{CO_2,g,o}$  and incident irradiance  $G_{in}$  while  $G_{av}$  and  $C_{TOT}$  are allowed to vary with time.

*CO<sub>2</sub> consumption*

Figure 3(a) shows the evolution of the CO<sub>2</sub> molar fraction  $x_{CO_2,g}$  in the head-space as a function of time  $t$ , normalized with the initial CO<sub>2</sub> mole fraction  $x_{CO_2,g,0}$  for different combinations of the total incident irradiance  $G_{in}$  and  $x_{CO_2,g,0}$ . It indicates that  $x_{CO_2,g}$  decreases monotonically with increasing time. First, the half-time, denoted by  $t_{1/2}$ , is defined as the time required for the CO<sub>2</sub> mole fraction in the gas phase to decrease to half of its initial value. Normalizing the time by the half-time and plotting the dimensionless variables  $x_{CO_2,g}/x_{CO_2,g,0}$  vs  $t/t_{1/2}$ , collapses all the data points to a single line as shown in Fig. 3(b). This

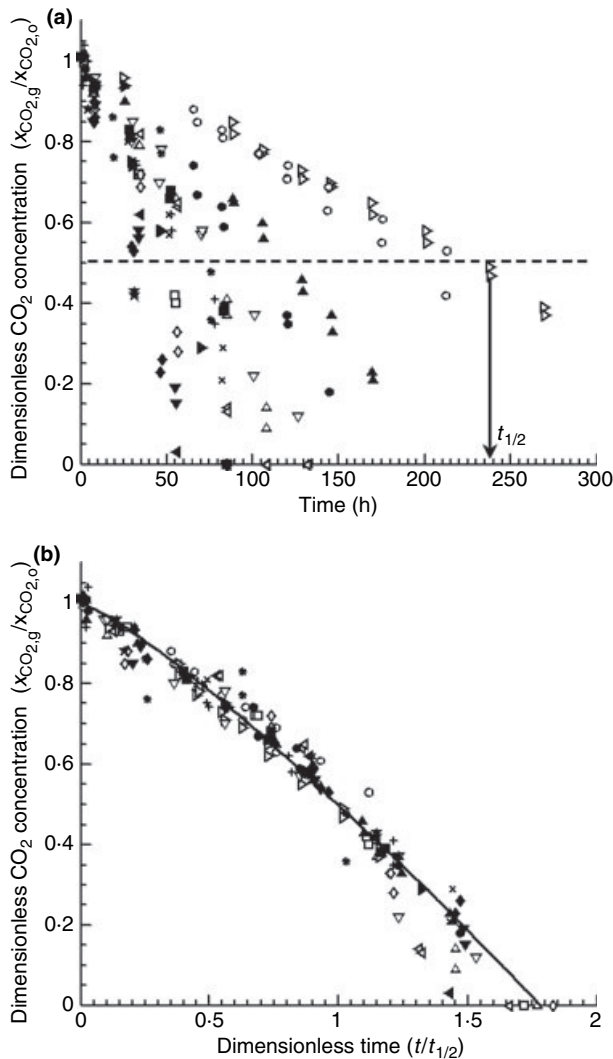


**Figure 3** (a) Normalized CO<sub>2</sub> consumption data vs time, (b) normalized CO<sub>2</sub> consumption data vs dimensionless time for (Δ) 0GH, (◁) 0IJ, (▷) 1AB, (○) 1CD, (▽) 1EF, (□) 1GH, (◇) 1IJ, (▲) 2AB, (●) 2CD, (◄) 2EF, (▼) 2GH, (►) 2IJ, (■) 3AB, (×) 3CD, (◆) 3EF, (+) 4AB, (★) 4CD, (☆) 4EF. The solid line corresponds to  $x_{CO_2,g}/x_{CO_2,g,0} = 1 - 0.5(t/t_{1/2})^{1.2}$ .

indicates that the CO<sub>2</sub> consumption half time is an appropriate time scale for comparing CO<sub>2</sub> consumption under different conditions. Performing a linear regression analysis of the data yields:

$$\frac{x_{CO_2,g}}{x_{CO_2,g,0}} = 1 - 0.5 \left( \frac{t}{t_{1/2}} \right)^{1.2}, \quad (8)$$

with a correlation coefficient  $R^2=0.94$ . Equation (8) also indicates that  $x_{CO_2,g}$  vanishes at time  $t=1.8t_{1/2}$ .

Moreover, the half-time  $t_{1/2}$  is a function of both the initial CO<sub>2</sub> mole fraction and the irradiance  $G_{in}$ . Figure 4(a) shows  $t_{1/2}$  as a function of  $x_{CO_2,g,0}$  for different values of  $G_{in}$ . It indicates that  $t_{1/2}$  increases linearly with  $x_{CO_2,g,0}$  for a given  $G_{in}$ , i.e.  $t_{1/2} = \beta(G_{in})x_{CO_2,g,0}$ , where the slope  $\beta(G_{in})$  is expressed in hours and plotted in Fig. 4(b). Two regimes can be identified. In the first regime,  $\beta(G_{in})$  decreases linearly with  $G_{in}$  according to  $\beta(G_{in}) = 1900 - 0.3G_{in}$ . In the second regime,  $\beta(G_{in})$  does not vary appreciably with  $G_{in}$  and has the approximate value of 350 h. Figure 4(b) indicates that transition between the two regimes occurs around  $G_{in} = 5170$  lux. Therefore, the half-time  $t_{1/2}$  can be expressed as:

$$\begin{aligned} t_{1/2} &= (1900 - 0.3G_{in})x_{CO_2,g,0} \quad \text{for } G_{in} \leq 5170 \text{ lux} \\ t_{1/2} &= 350x_{CO_2,g,0} \quad \text{for } G_{in} > 5170 \text{ lux} \end{aligned} \quad (9)$$

Alternatively, the relationship between  $\beta$  and  $G_{in}$  can be approximated with an exponential decay function as  $\beta(G_{in}) = 350 + 1300\exp(9 \times 10^{-8}G_{in}^2)$ .

Furthermore, Fig. 5(a) compares the values of experimentally determined  $t_{1/2}$  with those predicted by eqn (9). With the exception of one outlier, all the experimentally determined half-times lie within  $\pm 20$  h of the predictions by eqn (9). The experimental values of  $t_{1/2}$  and  $t_d$  are summarized in Table 2 for each test.

In addition, Fig. 5(b) shows the medium pH as a function of the dimensionless time  $t/t_{1/2}$  for all runs. It shows that the medium pH increases as the CO<sub>2</sub> is consumed by the micro-organisms. It also indicates that the pH changes also scale well with the time scale  $t_{1/2}$ .

*Cyanobacterial growth*

Figure 6(a,b) show the normalized concentration of *A. variabilis*,  $X/X_0$ , vs time  $t$  for all irradiances and for  $x_{CO_2,g,0} = 0.08$  and  $0.15$  respectively. The initial cyanobacteria concentration  $X_0$  is equal to  $0.02 \text{ kg dry cell m}^{-3}$  in all cases. Figure 6 establishes that for a given  $x_{CO_2,g,0}$ , increasing the irradiance increases the growth rate of *A. variabilis*. Moreover, for a given irradiance  $G_{in}$  within the values tested, decreasing the initial CO<sub>2</sub> mole fraction increases the growth rate. Thus, the effects of  $G_{in}$  and  $x_{CO_2,g,0}$  on cyanobacterial growth seem to be coupled.



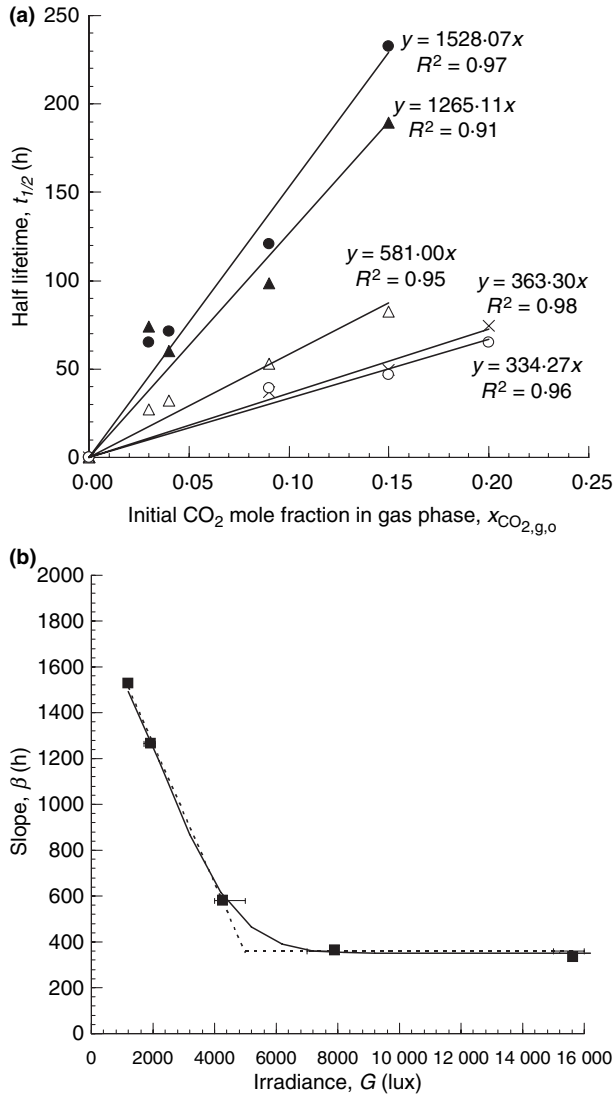


**Figure 4** (a) Half-time as a function of  $x_{CO_2,g,0}$  for (●) 1100–1200 lux, (▲) 1700–1800 lux, (△) 4000–5000 lux, (×) 7000–8000 lux, and (○) 15 000–16 000 lux. (b) Slope  $\beta$  as a function of irradiance  $G$ . The solid line corresponds to  $\beta = 350 + 1300\exp(-9 \times 10^{-8}G^2)$ .

Here also, scaling the time with the half-time  $t_{1/2}$  collapses the growth curves for different irradiances onto a single line as shown in Fig. 6c,d for  $x_{CO_2,g,0} = 0.08$  and 0.15 respectively. Therefore, the half-time  $t_{1/2}$  correctly captures the time scale of the biological processes for CO<sub>2</sub> consumption and bacterial growth. In addition, the cyanobacterial growth is exponential and the cyanobacteria concentration  $X(t)$  at time  $t$  can be expressed as:

$$\frac{X(t)}{X_0} = \exp\left(\frac{\alpha}{t_{1/2}}t\right), \quad (10)$$

where  $\alpha$  is a constant depending on  $x_{CO_2,g,0}$  and determined experimentally. Figure 7 shows its evolution as a

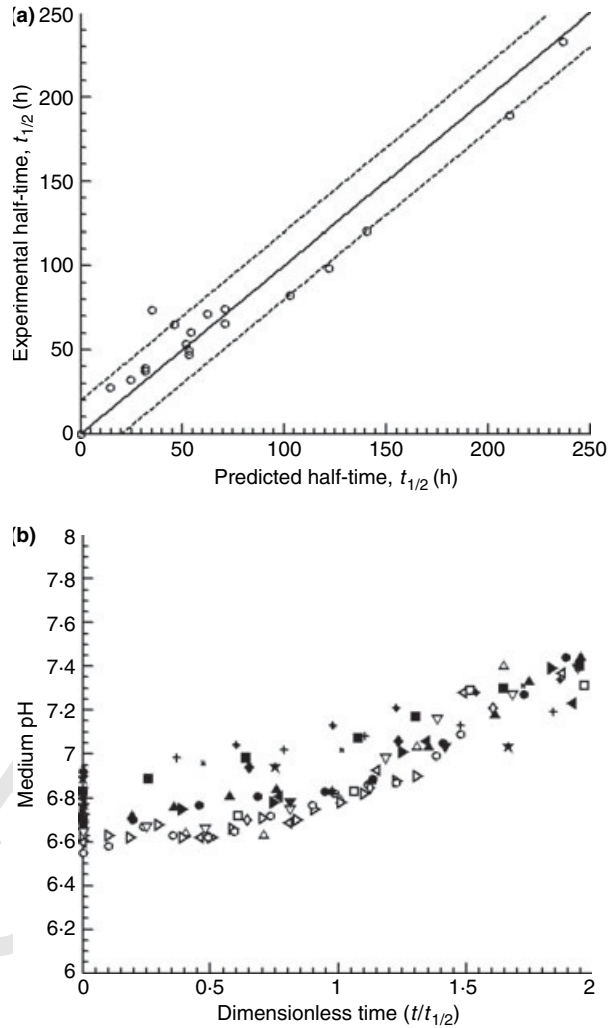


**Figure 5** (a) Comparison of experimental vs predicted half-times. The solid line corresponds to the model  $t_{1/2} = (1900 - 0.3G)x_{CO_2,g,0}$  and the dashed lines correspond to  $\pm 20\%$ -hdeviations from the model. (b) The medium pH as a function of the dimensionless time  $t/t_{1/2}$  for (△) 0GH, (◁) 0IJ, (▷) 1AB, (○) 1CD, (▽) 1EF, (□) 1GH, (◇) 1IJ, (▲) 2AB, (●) 2CD, (◀) 2EF, (▼) 2GH, (▶) 2IJ, (■) 3AB, (×) 3CD, (◆) 3EF, (+) 4AB, (★) 4CD, (☆) 4EF.

function of  $x_{CO_2,g,0}$  varying between 0.03 and 0.20. The relationship can be expressed as:

$$\alpha = 4x_{CO_2,g,0}^{0.35} \quad (11)$$

with a correlation coefficient  $R^2 = 0.93$ . Note that the evolution of  $X(t)$  as a function of the irradiance  $G_{in}$  and  $x_{CO_2,g,0}$  is accounted for through the half-time  $t_{1/2}$  given by eqn (9).

Moreover, the average specific growth rate, denoted by  $\mu_{avg}$ , is the arithmetic mean of the specific growth rates, denoted by  $\mu_{\Delta t}$  and determined in the time interval  $\Delta t$

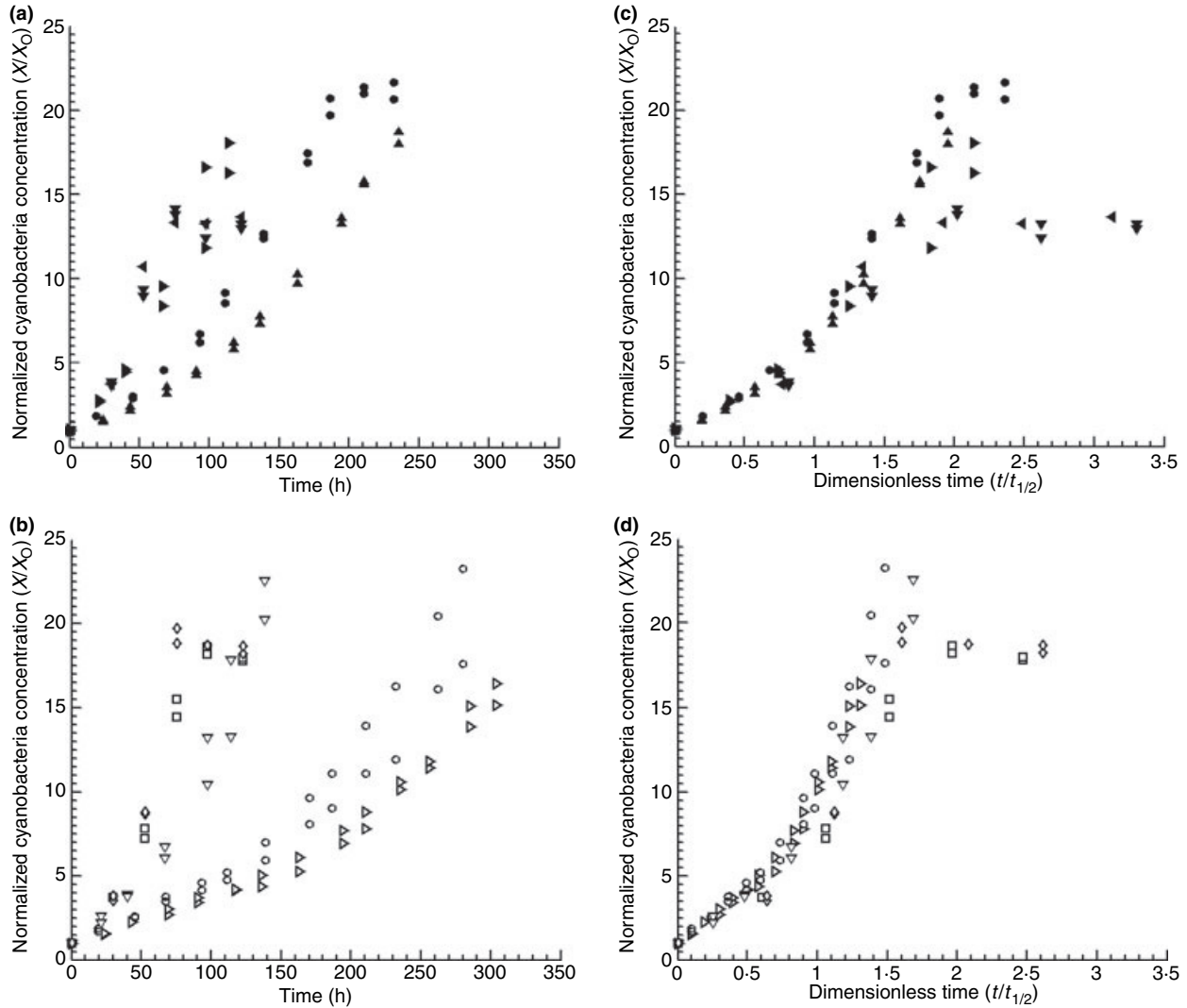


**Figure 6** Normalized cyanobacteria concentrations at all irradiances as functions of time for (a)  $x_{CO_{2,9,0}}=0.08$  and (b)  $x_{CO_{2,9,0}}=0.15$ . Normalized cyanobacteria concentrations at all irradiances as functions of dimensionless time for (c)  $x_{CO_{2,9,0}}=0.08$  and (d)  $x_{CO_{2,9,0}}=0.15$  for (▲) 2AB, (●) 2CD, (□) 2EF, (▼) 2GH, (◀) 2IJ, (▷) 1AB, (○) 1CD, (▽) 1EF, (◻) 1GH, (◇) 1IJ.

during the exponential growth phase of *A. variabilis* according to (Yoon et al. 2002):

$$\mu_{\Delta t} = \frac{\Delta X}{\Delta t} \frac{1}{X_{avg,\Delta t}}, \quad (12)$$

where  $X_{avg,\Delta t}$  is the arithmetic mean of the cyanobacteria concentration during that time interval  $\Delta t$ . The values of  $\mu_{avg}$  computed for all parameters are summarized in Table 2. Figure 12(a) presents the variation of the average specific growth rate of *A. variabilis* denoted by  $\mu_{avg}$  and expressed in  $h^{-1}$ , as a function of  $x_{CO_{2,9,0}}$  for all irradiances. The error bars indicate the standard error that is the ratio of the standard deviation to the square root of the number of samples.

Furthermore, the average specific CO<sub>2</sub> uptake rate, denoted by  $\psi_{CO_2}$  and expressed in  $kg\ kg^{-1}\ dry\ cell\ h^{-1}$ , is computed using the same method as that used by Yoon et al. (2002):

$$\psi_{CO_2} = \frac{\mu_{avg}}{Y_{X/CO_2}}, \quad (13)$$

where  $Y_{X/CO_2}$  is the biomass yield based on consumed CO<sub>2</sub> expressed in  $kg\ dry\ cell\ kg^{-1}$  of CO<sub>2</sub>. It is computed as the ratio of the final mass of cyanobacteria produced to the total mass of CO<sub>2</sub> injected into the vials. The values of  $\psi_{CO_2}$  computed for all parameters are also summarized in Table 2. Figure 12(b) shows the variation of  $\psi_{CO_2}$  as a function of  $x_{CO_{2,9,0}}$  for all irradiances.

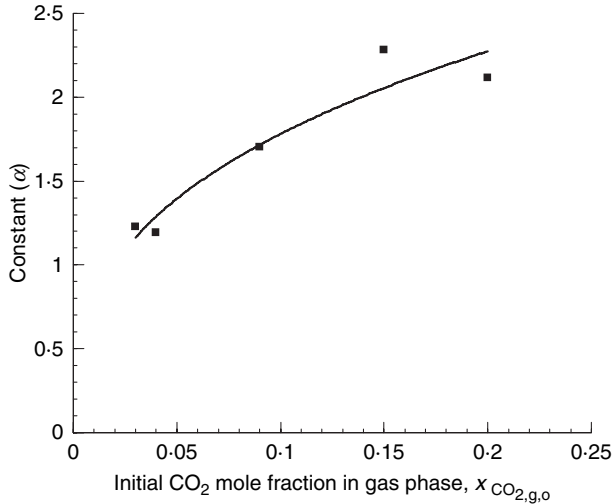


**Figure 7** (a) The constant  $\alpha$  in eqn (10) as a function of  $x_{\text{CO}_2,\text{g},0}$ . The solid line corresponds to  $\alpha = 4x_{\text{CO}_2,\text{g},0}^{0.35}$ .

#### Hydrogen and oxygen productions

Figure 9(a) shows the concentration of hydrogen measured in the head-space as a function of the dimensionless time  $t/t_{1/2}$  for all runs. It indicates that the maximum hydrogen concentration is achieved at high irradiance. Moreover, the concentration of hydrogen accumulated in the head-space normalized with its maximum value  $C_{\text{H}_2,\text{g},\text{max}}$  as a function of dimensionless time  $t/t_{1/2}$  for irradiance larger than 7000 lux is shown in Fig. 9b. It establishes that  $C_{\text{H}_2,\text{g}}/C_{\text{H}_2,\text{g},\text{max}}$  varies exponentially with  $t/t_{1/2}$  and can be expressed as:

$$\frac{C_{\text{H}_2,\text{g}}(t)}{C_{\text{H}_2,\text{g},\text{max}}} = \exp \left[ 4.45 \left( \frac{t}{t_{1/2}} \right) - 6.1 \right] \quad (14)$$

Similarly, Fig. 10(a,b) show the oxygen concentration and the normalized oxygen concentration with its maximum value, respectively, as functions of the dimensionless time  $t/t_{1/2}$  for all runs. Figure 10(b) indicates that the normalized oxygen concentration varies exponentially with  $t/t_{1/2}$  according to:

$$\frac{C_{\text{O}_2,\text{g}}(t)}{C_{\text{O}_2,\text{g},\text{max}}} = \exp \left[ 2.25 \left( \frac{t}{t_{1/2}} \right) - 3.5 \right] \quad (15)$$

To use eqns (14) and (15) to determine the evolution of oxygen and hydrogen concentrations, the maximum concentrations  $C_{\text{O}_2,\text{g},\text{max}}$  and  $C_{\text{H}_2,\text{g},\text{max}}$  must be expressed in terms of the initial CO<sub>2</sub> mole fraction  $x_{\text{CO}_2,\text{g},0}$  and irradiance  $G$ . Figure 11 shows that  $C_{\text{O}_2,\text{g},\text{max}}$  is independent of irradiance and varies linearly with  $x_{\text{CO}_2,\text{g},0}$  according to:

$$C_{\text{O}_2,\text{g},\text{max}} = 3.45x_{\text{CO}_2,\text{g},0} \quad (16)$$

with a correlation coefficient  $R^2=0.94$ . This demonstrates that the oxygen yield of *A. variabilis*, i.e. the mass of O<sub>2</sub> produced per mass of CO<sub>2</sub> consumed, was constant for the parameters explored.

Figure 12(a) shows  $C_{\text{H}_2,\text{g},\text{max}}$  as a function of both irradiance and of the initial CO<sub>2</sub> mole fraction. It indicates that within the parameter ranges explored, the optimum irradiance for maximum H<sub>2</sub> production was around 10 000 lux. Figure 12(b) shows  $C_{\text{H}_2,\text{g},\text{max}}$  as a function of  $x_{\text{CO}_2,\text{g},0}$  for irradiances larger than 7000 lux for which H<sub>2</sub> production is the largest. It indicates that  $C_{\text{H}_2,\text{g},\text{max}}$  increases with increasing  $x_{\text{CO}_2,\text{g},0}$ . As a first order approximation, the relationship between  $C_{\text{H}_2,\text{g},\text{max}}$  and  $x_{\text{CO}_2,\text{g},0}$  can be written as:

$$C_{\text{H}_2,\text{g},\text{max}} = 1.50 \times 10^{-2}x_{\text{CO}_2,\text{g},0} - 3.75 \times 10^{-4} \quad (17)$$

for  $G \geq 7000$  lux

with a correlation coefficient  $R^2$  of 0.75.

#### Discussion

Kinetic models describing the cyanobacterial growth, carbon uptake, and O<sub>2</sub> production depend on the specific growth rate  $\mu$  which is a function of the instantaneous available irradiance  $G_{\text{av}}$  and total dissolved inorganic carbon concentration  $C_{\text{TOT}}$ . In an earlier study, Badger and Andrews (1982) suggested that both H<sub>2</sub>CO<sub>3</sub><sup>\*</sup> and HCO<sub>3</sub><sup>-</sup> can act as substrate for cyanobacteria. Furthermore, Goldman *et al.* (1974) used  $C_{\text{TOT}}$  given by eqn (5) in the Monod model to successfully predict algal growth in carbon limited conditions for pH between 7.05 and 7.61. More recently, Erickson *et al.* (1987) modelled the growth rate of the cyanobacteria *S. platensis* under light and inorganic carbon limited conditions using the Monod model. Table 3 indicates that the parameters they reported for *S. platensis* agree well with those obtained in the present study for *A. variabilis*. Note that Erickson *et al.* (1987) expressed the Monod model only in terms of HCO<sub>3</sub><sup>-</sup> concentration as opposed to  $C_{\text{TOT}}$ . However, it is equivalent to using  $C_{\text{TOT}}$  as the pH was kept constant and equal to 9.2. Then, the ratio of HCO<sub>3</sub><sup>-</sup> to H<sub>2</sub>CO<sub>3</sub><sup>\*</sup> concentrations is about 800 while CO<sub>3</sub><sup>2-</sup> concentration is negligibly small. In other words, at pH 9.2,  $C_{\text{TOT}}$  is approximately equal to the HCO<sub>3</sub><sup>-</sup> concentration. In the present study, the pH varies from 6.6 to 7.4 and the ratio of HCO<sub>3</sub><sup>-</sup> to H<sub>2</sub>CO<sub>3</sub><sup>\*</sup> concentration varies between 2 and 12. Therefore, both species need to be accounted for in computing  $C_{\text{TOT}}$  to be used in eqn (2). Furthermore, the aforementioned studies did not account for the inhibitory effect of dissolved inorganic carbon (i.e.  $K_I = \infty$ ) as the

concentration of inorganic carbon was low,  $C_{TOT} < 0.67 \times 10^{-3} \text{ kmol C m}^{-3}$ . However, in the present study, the inorganic carbon concentration reached up to  $C_{TOT} < 20 \times 10^{-3} \text{ kmol C m}^{-3}$  and ignoring the carbon inhibition effects in eqn (2) resulted in poor model predictions. The values of the retrieved parameters  $\mu_{max}$ ,  $K_G$ , and  $K_C$  agree with those reported by Erickson *et al.* (1987) and are valid for low carbon concentrations. In addition, the inhibitory effect of large inorganic carbon concentration is successfully accounted for by the modified Monod model through the parameter  $K_I$ .

Moreover, due to the fact that CO<sub>2</sub> consumption and O<sub>2</sub> production are mainly growth related processes, their evolution has been successfully modelled using the specific growth rates. On the other hand, H<sub>2</sub> evolution is a much more complex process. It depends on the active enzyme concentration, the O<sub>2</sub> concentration in the medium, the irradiance, as well as the growth rate. Therefore, simple models similar to eqns (6) or (7) could not model all data within  $\pm 30\%$ .

Furthermore, these models assume that the irradiance within the culture and the concentration of the dissolved inorganic carbon are known while they cannot be measured directly. Consequently, in the second part of this paper a new analysis for CO<sub>2</sub> consumption, cyanobacterial growth, as well as hydrogen and oxygen productions as functions of  $t_{1/2}$  has been developed. Experimental data indicates that  $t_{1/2}$  is a relevant time scale for CO<sub>2</sub> consumption, growth, H<sub>2</sub> and O<sub>2</sub> production. The simplicity of this analysis resides in the fact that it depends on directly measurable and controllable quantities. Furthermore, it can be used to determine the light saturation of photosynthesis as shown in Fig. 4. However, the applicability of this scaling analysis is limited to systems having (i) the same initial cyanobacteria concentration and (ii) similar pH.

Moreover, Fig. 12(a) establishes that an optimum  $x_{CO_{2,g,o}}$  around 0.05 exists for maximum average specific growth rate for all irradiances. Moreover, it shows that the average specific growth rate increases with increasing irradiance. Yoon *et al.* (2002) reported that for experiments conducted at 30°C with  $x_{CO_{2,g,o}}$  around 0.11 the average specific growth rate decreased from 0.054 to 0.046 h<sup>-1</sup> for *A. variabilis* as the irradiance increased from 3500 to 7000 lux. In the present study at 24°C with initial CO<sub>2</sub> mole fraction of 0.11,  $\mu_{avg}$  increased from 0.028 to 0.038 h<sup>-1</sup> for the same increase in irradiance. The observed discrepancy between the results reported in this study and those reported by Yoon *et al.* (2002) can be attributed to the combination of the differences in pH and in temperature.

Furthermore, Fig. 8b shows that the average specific CO<sub>2</sub> uptake rate exhibits similar trends to those of the

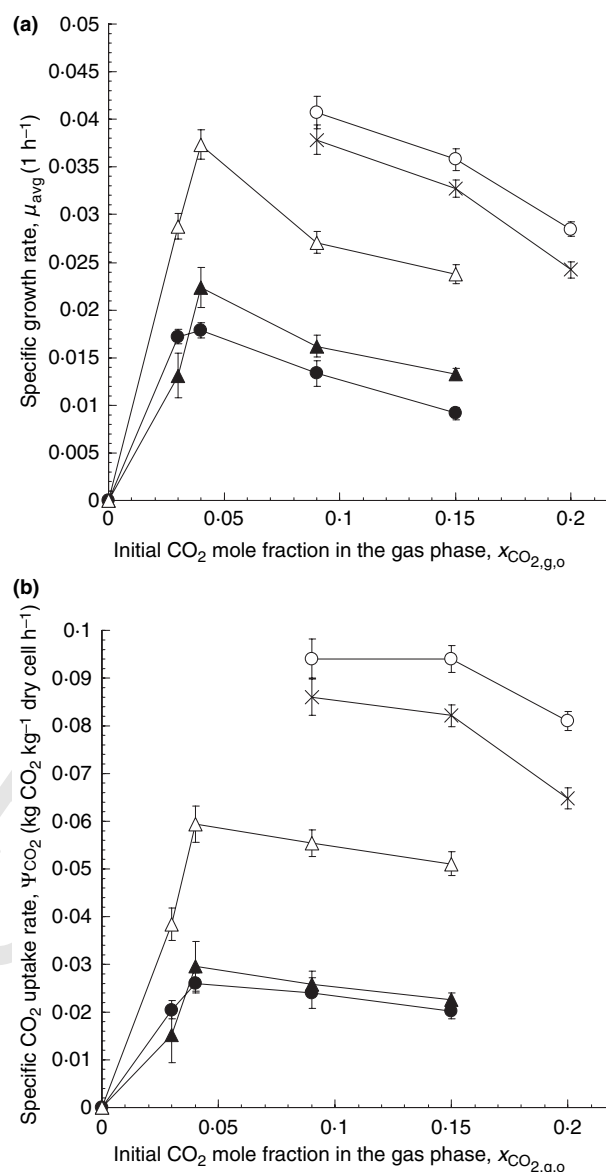


**Figure 8** (a) The average specific growth rate  $\mu_{avg}$ , and (b) the average specific CO<sub>2</sub> uptake rate  $\psi_{CO_2}$  of *Anabaena variabilis* as functions of  $x_{CO_{2,g,o}}$  at all irradiances: (●) 1100–1200 lux, (▲) 1700–1800 lux, (△) 4000–5000 lux, (×) 7000–8000 lux and (○) 15 000–16 000 lux.

average specific growth rate with an optimum  $x_{CO_{2,g,o}}$  around 0.05 for maximum  $\psi_{CO_2}$ . Yoon *et al.* (2002) reported an average specific CO<sub>2</sub> uptake rate  $\psi_{CO_2}$  of about 0.130 kg CO<sub>2</sub> kg<sup>-1</sup> dry cell h<sup>-1</sup> for  $x_{CO_{2,g,o}}$  around 0.05 and irradiance around 4000 lux, whereas, in the present study, it was only 0.060 kg CO<sub>2</sub> kg<sup>-1</sup> dry cell h<sup>-1</sup> under the same irradiance and  $x_{CO_{2,g,o}}$ . The difference can be attributed to the fact that the experiments of the present study were conducted at 24°C instead of 30°C (Yoon *et al.* 2002). It is apparent that increasing

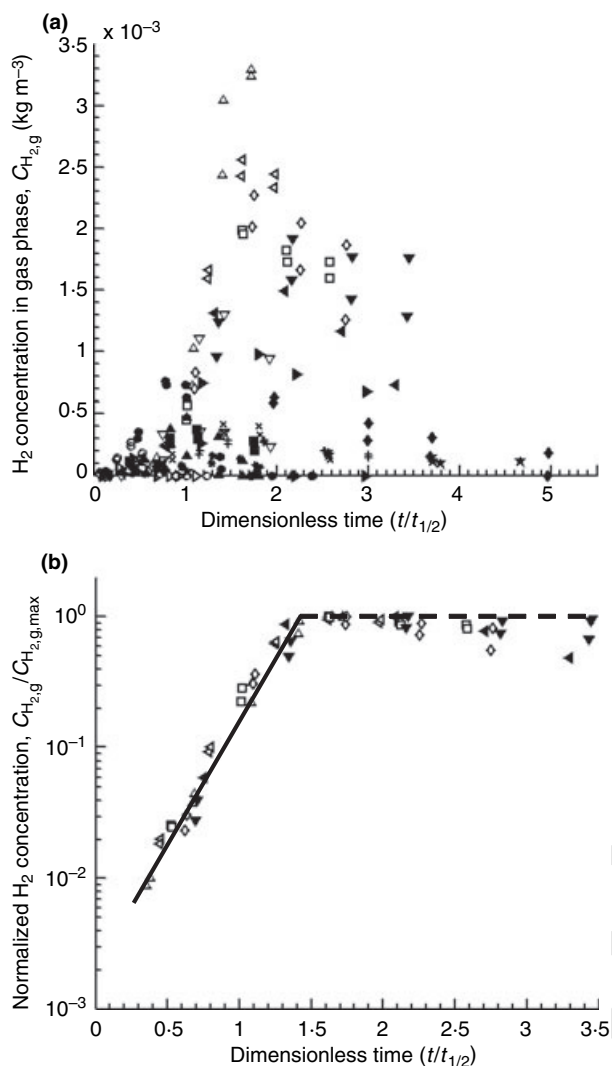


**Figure 9** Concentration of hydrogen accumulated in the head-space (a) for all tests vs dimensionless time  $t/t_{1/2}$ , (b) normalized with the maximum concentration produced vs dimensionless time  $t/t_{1/2}$  for irradiance  $G \geq 7000$  lux. The solid line corresponds to  $C_{H_2,g}/C_{H_2,g,max} = \exp[4.45(t/t_{1/2}) - 6.1]$ . ( $\Delta$ ) 0GH, ( $\triangleleft$ ) 0IJ, ( $\triangleright$ ) 1AB, ( $\circ$ ) 1CD, ( $\nabla$ ) 1EF, ( $\square$ ) 1GH, ( $\diamond$ ) 1IJ, ( $\blacktriangle$ ) 2AB, ( $\bullet$ ) 2CD, ( $\blacktriangleleft$ ) 2EF, ( $\blacktriangledown$ ) 2GH, ( $\blacktriangleright$ ) 2IJ, ( $\blacksquare$ ) 3AB, ( $\times$ ) 3CD, ( $\blacklozenge$ ) 3EF, ( $+$ ) 4AB, ( $\star$ ) 4CD, ( $\star$ ) 4EF.

the temperature enhances the CO<sub>2</sub> uptake metabolism of *A. variabilis* as confirmed by Tsygankov *et al.* (1999). Note that due to experimental difficulties in capturing fast CO<sub>2</sub> consumption rate with the available equipment and procedure, no experiments were conducted for initial CO<sub>2</sub> mole fraction less than 0.08 at irradiances higher than 5000 lux.

Figures 9 and 10 show that H<sub>2</sub> and O<sub>2</sub> concentrations in the headspace increases exponentially during the growth phase. Due to the presence of nitrate in the medium (initially about 20 mmol l<sup>-1</sup>), the nitrogenase activity is expected to be low (Madamwar *et al.* 2000). Moreover,

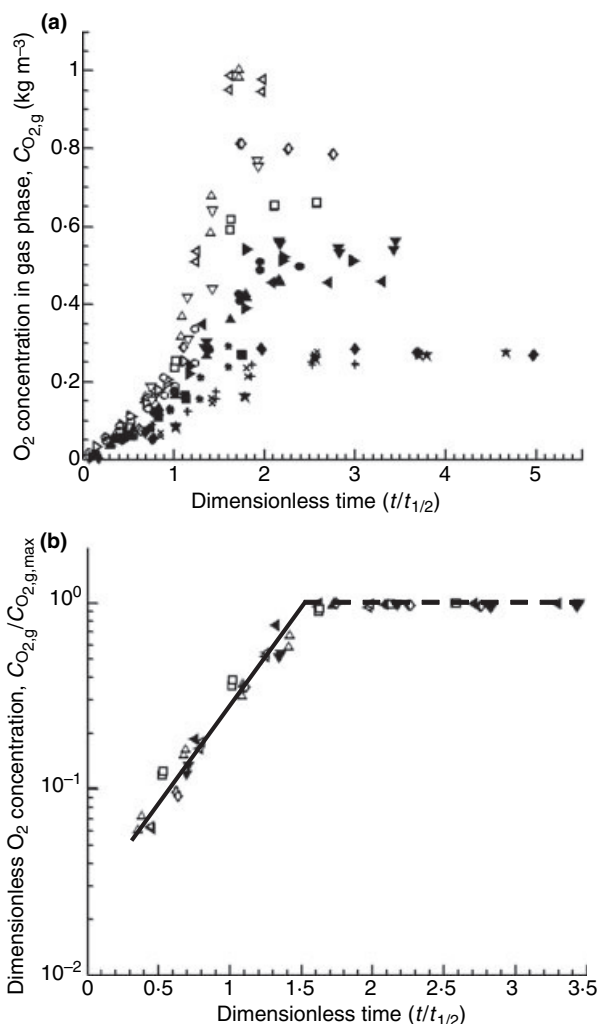


**Figure 10** Concentration of oxygen accumulated in the head-space for (a) all tests vs dimensionless time  $t/t_{1/2}$ , (b) normalized with the maximum concentration produced vs dimensionless time  $t/t_{1/2}$  for irradiance  $G \geq 7000$  lux. The solid line corresponds to  $C_{O_2,g}/C_{O_2,g,max} = \exp[2.25(t/t_{1/2}) - 3.5]$ . ( $\Delta$ ) 0GH, ( $\triangleleft$ ) 0IJ, ( $\triangleright$ ) 1AB, ( $\circ$ ) 1CD, ( $\nabla$ ) 1EF, ( $\square$ ) 1GH, ( $\diamond$ ) 1IJ, ( $\blacktriangle$ ) 2AB, ( $\bullet$ ) 2CD, ( $\blacktriangleleft$ ) 2EF, ( $\blacktriangledown$ ) 2GH, ( $\blacktriangleright$ ) 2IJ, ( $\blacksquare$ ) 3AB, ( $\times$ ) 3CD, ( $\blacklozenge$ ) 3EF, ( $+$ ) 4AB, ( $\star$ ) 4CD, ( $\star$ ) 4EF.

H<sub>2</sub> production using the nitrogenase enzyme is not expected to stop when the growth stops or slows down such as during two stage H<sub>2</sub> production (Yoon *et al.* 2002). However, increased concentration of evolved O<sub>2</sub> could have inhibited H<sub>2</sub> production. In addition, the initial anaerobic conditions promotes the bidirectional hydrogenase activity. Therefore, the observed H<sub>2</sub> production during the experiments is expected to be due to the bidirectional hydrogenase activity. Furthermore, the decrease in the H<sub>2</sub> concentration for  $t/t_{1/2} > 1.5$  can be attributed to consumption of the produced H<sub>2</sub> due to the presence of uptake hydrogenase (Tsygankov *et al.* 1998).

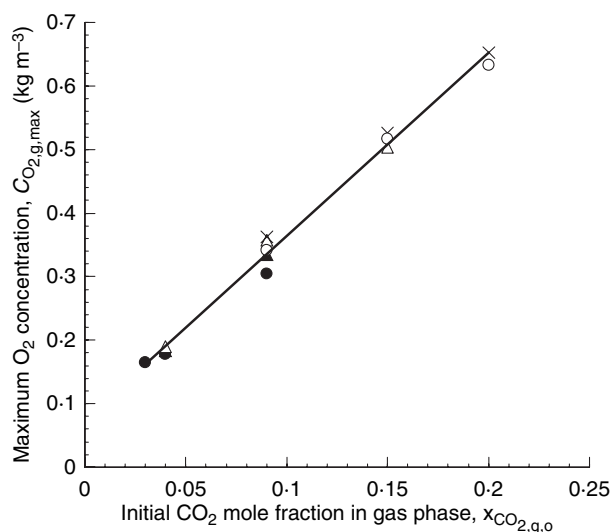


**Figure 11** Maximum concentration of oxygen accumulated in the head-space  $C_{O_2,g,max}$  as a function of the  $x_{CO_2,g,o}$  for (●) 1100–1200 lux, (▲) 1700–1800 lux, (△) 4000–5000 lux, (×) 7000–8000 lux and (○) 15 000–16 000 lux. The solid line corresponds to  $C_{O_2,g,max} = 3.45x_{CO_2,g,o}$ .

However, unlike hydrogen, the oxygen concentration does not decrease appreciably beyond the exponential growth phase. Finally,  $C_{H_2,g}$  and  $C_{O_2,g}$  reach their maximum at dimensionless time  $t/t_{1/2}$  equal to 1.37 and 1.55, respectively, and shortly before the CO<sub>2</sub> concentration vanishes at  $t/t_{1/2}$  equal to 1.8. Note that the reported values of CO<sub>2</sub>, O<sub>2</sub>, and H<sub>2</sub> values correspond to the net produced or consumed quantities as it is difficult to experimentally distinguish the contribution of each phenomenon. In particular, CO<sub>2</sub> is being consumed during photosynthesis and being produced during respiration and possibly during H<sub>2</sub> production, provided H<sub>2</sub> production is catalyzed by nitrogenase (Das and Veziroglu 2001). Similarly, O<sub>2</sub> is being produced during photosynthesis and consumed during respiration.

Figures 11 and 12 show the maximum O<sub>2</sub> and H<sub>2</sub> concentrations attained in the headspace as functions of  $x_{CO_2,g,o}$  for different irradiances. Unlike for  $C_{O_2,g,max}$ , it is difficult to establish a simple and reliable relationship between  $C_{H_2,g,max}$  and the parameters  $G$  and  $x_{CO_2,g,o}$  due to the complexity of the hydrogen metabolism of *A. variabilis*. This complexity arises because (i) the hydrogen production is a strong function of both the irradiance  $G$  and the initial CO<sub>2</sub> concentration (Markov *et al.* 1997a) and (ii) the produced hydrogen is being consumed back by the micro-organisms at a rate comparable to the production rate of hydrogen (Tsygankov *et al.* 1998). Tsygankov *et al.* (1998) reported that the wild strain *A. variabilis* ATCC 29413 did not produce any hydrogen in the pres-

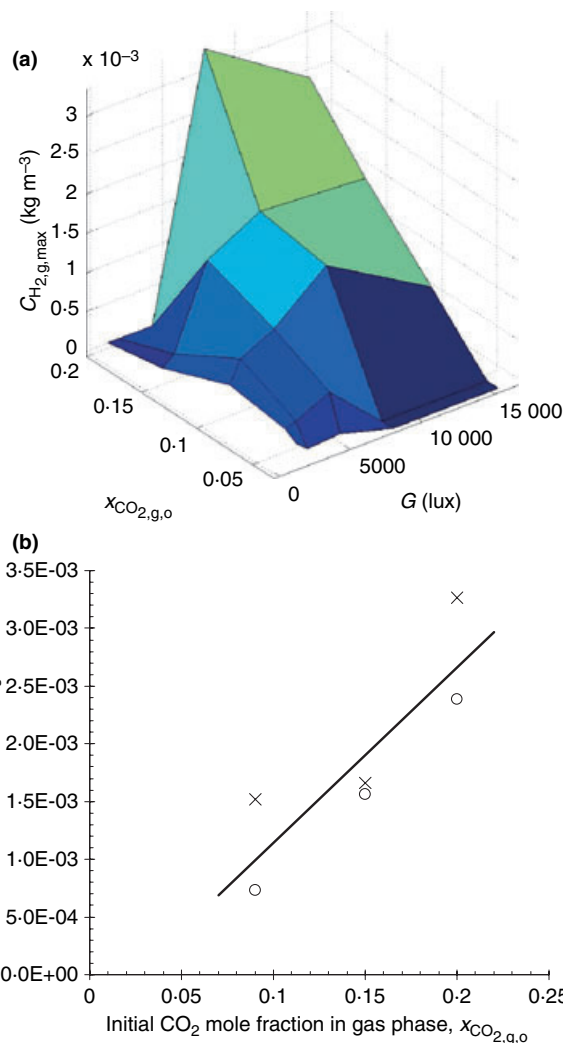


**Figure 12** (a) Maximum concentration of hydrogen accumulated in the head-space as a function of the initial CO<sub>2</sub> mole fraction and irradiance. (b)  $C_{H_2,g,max}$  as a function of  $x_{CO_2,g,o}$  for two of the highest irradiances for (×) 7,000–8,000 lux and (○) 15 000–16 000 lux. The solid line corresponds to  $C_{H_2,g,max} = 1.50 \times 10^{-2}x_{CO_2,g,o} - 3.75 \times 10^{-4}$ .

ence of CO<sub>2</sub> in the atmosphere. In contrast, the present study indicates that hydrogen production by the wild strain is possible under argon and CO<sub>2</sub> atmosphere albeit at a lower production rate. Indeed, the maximum hydrogen production observed in our experiments was 0.3 mmol kg<sup>-1</sup> dry cell h<sup>-1</sup> whereas reported rates for wild *A. variabilis* strains range from 5.58 mmol kg<sup>-1</sup> dry cell h<sup>-1</sup> in dark fermentation (Shah *et al.* 2001), 165 mmol kg<sup>-1</sup> dry cell h<sup>-1</sup> in a multi stage photobioreactor (Yoon *et al.* 2006), and to 720 mmol kg<sup>-1</sup> dry cell h<sup>-1</sup> under nutritional stress (Sveshnikov *et al.* 1997). The low hydrogen production rates observed in the present study are attributed to (i) CO<sub>2</sub> fixation and H<sub>2</sub> production pro-

cesses competing for the reductants generated from water splitting (Prince and Kheshgi 2005); (ii) the presence of nitrate in the medium (Shah *et al.* 2001); and (iii) the consumption of the produced H<sub>2</sub> by the wild strain *A. variabilis* at high dissolved O<sub>2</sub> concentrations (Tsyganov *et al.* 1998).

## Conclusions

A parametric experimental study has been performed to assess the CO<sub>2</sub> consumption, growth, H<sub>2</sub> and O<sub>2</sub> productions of the cyanobacteria *A. variabilis* ATCC 29413-U<sup>TM</sup> in batch experiment. The main parameters are the irradiance and the initial CO<sub>2</sub> mole fraction in the head-space. The micro-organisms were grown in atmosphere containing argon and CO<sub>2</sub>, at a pH of 7.0 ± 0.4 with nitrate in the medium. A new scaling analysis for CO<sub>2</sub> consumption, growth, and H<sub>2</sub> and O<sub>2</sub> production is presented. Under the conditions presented in this study, the following conclusions can be drawn for *A. variabilis*,

1. Kinetic equations based on the Monod model are used to model the growth, carbon uptake, and O<sub>2</sub> production by *A. variabilis* taking into account (i) light saturation; (ii) CO<sub>2</sub> saturation; and (iii) CO<sub>2</sub> inhibition. The parameters obtained agree well with values reported for other cyanobacteria (Erickson *et al.* 1987) at low inorganic carbon concentrations and expands the model to large concentrations when growth inhibition occurs. The experimental data falls within 30% of the model predictions. However, similar approach could not predict experimental data for H<sub>2</sub> production rate.
2. The CO<sub>2</sub> consumption half-time, defined as the time when the CO<sub>2</sub> mole fraction in the gas phase decreases to half of its initial value, is a relevant time scale for CO<sub>2</sub> consumption, growth, H<sub>2</sub> and O<sub>2</sub> production. It depends on the total irradiance incident on the vials and the initial CO<sub>2</sub> mole fraction.
3. The scaling analysis facilitates the determination of the saturation irradiance which is found to be 5170 lux.
4. For maximum specific CO<sub>2</sub> consumption and specific growth rates, the optimum initial CO<sub>2</sub> mole fraction in the gas phase is about 0.05 for any irradiance between 1000 and 16 000 lux.
5. Optimum irradiance for maximum H<sub>2</sub> production has been found to be around 10 000 lux despite the low overall H<sub>2</sub> production rates.
6. Neither the CO<sub>2</sub> consumption nor the growth rate was inhibited by irradiance up to about 16 000 lux.

Finally, the kinetic equations can be used in simulations for optimizing the operating conditions of a photobioreactor for rapid growth and maximum CO<sub>2</sub> mitigation. Moreover, it is expected that the above experimental and scaling analysis method can be used for

analyzing other CO<sub>2</sub> mitigating and H<sub>2</sub> producing micro-organisms.

## Acknowledgements

The authors gratefully acknowledge the support of the California Energy Commission through the Energy Innovation Small Grant (EISG 53723A/03-29; Project Manager: Michelle McGraw). They are indebted to Chu Ching Lin, Edward Ruth, Jong Hyun Yoon, and Dr James C. Liao for their helpful discussions and exchanges of information.

## Nomenclature

$C$ ,	volumetric mass concentration, kg m <sup>-3</sup> ;
$C_{\text{TOT}}$ ,	molar concentration of total dissolved inorganic carbon, kmol m <sup>-3</sup> ;
$E_{\text{ext},\lambda}$ ,	spectral extinction cross-section, m <sup>2</sup> kg <sup>-1</sup> dry cell;
$E_{\text{ext,PAR}}$ ,	average extinction cross-section over the PAR, m <sup>2</sup> kg <sup>-1</sup> dry cell;
$G$ ,	local irradiance, lux;
$G_{\text{av}}$ ,	average irradiance within the culture in the spectral range from 400 to 700 nm, lux;
$G_{\text{in}}$ ,	total incident irradiance in the spectral range from 400 to 700 nm, lux;
$K_C$ ,	half-saturation constant for dissolved inorganic carbon, kmol m <sup>-3</sup> ;
$K_G$ ,	half-saturation constant for light, lux;
$K_I$ ,	inhibition constant for dissolved inorganic carbon, kmol m <sup>-3</sup> ;
$L$ ,	depth of the cyanobacteria suspension in the vial, m;
OD,	optical density;
$t$ ,	time, h;
$t_{1/2}$ ,	half-time, h;
$X$ ,	cyanobacteria concentration, kg dry cell m <sup>-3</sup> ;
$X_{\text{avg},\Delta t}$ ,	average cyanobacteria concentration in the time interval $\Delta t$ , kg dry cell m <sup>-3</sup> ;
$x$ ,	mole fraction;
$Y_{X/C}$ ,	biomass yield based on carbon, kg dry cell kmol <sup>-1</sup> C;
$Y_{X/\text{CO}_2}$ ,	biomass yield based on CO <sub>2</sub> , kg dry cell kg <sup>-1</sup> CO <sub>2</sub> ;
$Y_{\text{O}_2/X}$ ,	O <sub>2</sub> yield based on biomass, kg O <sub>2</sub> kg <sup>-1</sup> dry cell;
$z$ ,	location in the cyanobacteria suspension measured from the liquid surface, m;

## Greek symbols

$\alpha$ ,	exponential constant;
$\beta$ ,	slope of half-time vs initial CO <sub>2</sub> mole fraction in the gas phase, h;
$\mu_{\Delta t}$ ,	specific growth rate in the time interval $\Delta t$ , 1 h <sup>-1</sup> ;
$\mu_{\text{avg}}$ ,	average specific growth rate, 1 h <sup>-1</sup> ;
$\mu_{\text{max}}$ ,	maximum specific growth rate, 1 h <sup>-1</sup> ;
$\psi_{\text{CO}_2}$ ,	average specific CO <sub>2</sub> uptake rate, kg CO <sub>2</sub> kg <sup>-1</sup> dry cell h <sup>-1</sup> ;

## Subscripts

CO <sub>2</sub> ,	refers to carbon dioxide;
g,	refers to gas phase;
H <sub>2</sub> ,	refers to hydrogen;
i,	refers to a gas species;
L,	refers to liquid phase;
max,	refers to the maximum amount of a gas species produced by the cyanobacteria;
O <sub>2</sub> ,	refers to oxygen;
o,	refers to initial conditions.

## References

- Asenjo, J. and Merchuk, J. (1995) *Bioreactor System Design*. New York, NY: Marcel Dekker.
- Badger, M. and Andrews, T. (1982) Photosynthesis and inorganic carbon usage by the marine cyanobacterium *Synechococcus* sp. *Plant Physiol* **70**, 517–523.
- Benemann, J. (2000) Hydrogen production by microalgae. *J Appl Phycol* **12**, 291–300.
- Benjamin, M. (2002) *Water Chemistry*. New York, NY: McGraw Hill.
- Berberoğlu, H. and Pilon, L. (2007). Experimental measurement of the radiation characteristics of hydrogen producing microorganisms. *Fifth International Symposium on Radiative Transfer*, Bodrum, Turkey, 17–22 June.
- 18 Berberoğlu, H., Yin, J. and Pilon, L. (2007) Simulating light transfer in a bubble sparged photobioreactor for simultaneous hydrogen fuel production and CO<sub>2</sub> mitigation. *Int J Hydrogen Energy* (in press).
- 19 Borodin, V., Tsygankov, A., Rao, K. and Hall, D. (2000) Hydrogen Production by *Anabaena variabilis* PK84 under simulated outdoor conditions. *Biotechnol Bioeng* **69**, 478–485.
- Das, D. and Veziroglu, T. (2001) Hydrogen Production by biological processes: a survey of literature. *Int J Hydrogen Energy* **26**, 13–28.
- Dunn, I., Heinzle, E., Ingham, J. and Prenosil, J. (2003) *Biological Reaction Engineering: Dynamic Modelling Fundamentals with Simulation Examples*, 2nd edn. Wiley-VCH, ?????.
- 20 of Energy, D. (2007). Joint Genome Institute. Available at: <http://www.jgi.doe.gov> (accessed on: April 19, 2007).
- 21 Erickson, L., Curless, C. and Lee, H. (1987) Modeling and simulation of photosynthetic microbial growth. *Ann NY Acad Sci* **506**, 308–324.
- Goldman, J., Oswald, W. and Jenkins, D. (1974) The kinetics of inorganic carbon limited algal growth. *J Water Pollut Control Fed* **46**, 554–574.
- Hansel, A. and Lindblad, P. (1998) Towards optimization of cyanobacteria as biotechnologically relevant producers of molecular hydrogen, a clean and renewable energy source. *Appl Microbiol Biotechnol* **50**, 153–160.
- Happe, T., Schutz, K. and Bohme, H. (2000) Transcriptional and mutational analysis of the uptake hydrogenase of the filamentous cyanobacterium *Anabaena variabilis* ATCC 29413. *J Biotechnol* **182**, 1624–1631.
- Madamwar, D., Garg, N. and Shah, V. (2000) Cyanobacterial hydrogen production World. *J Microbiol Biotechnol* **16**, 757–767.
- Markav, S., Lichtl, R., Rao, K. and Hall, D. (1993) A hollow fibre photobioreactor for continuous production of hydrogen by immobilized cyanobacteria under partial vacuum. *Int J Hydrogen Energy* **18**, 901–906.
- Markov, S., Bazin, M. and Hall, D. (1995) Hydrogen photoproduction and carbon dioxide uptake by immobilized *Anabaena variabilis* in a hollow-fiber photobioreactor. *Enzyme Microb Technol* **17**, 306–310.
- Markov, S., Thomas, A., Bazin, M. and Hall, D. (1997a) Photoproduction of hydrogen by cyanobacteria under partial vacuum in batch culture or in a photobioreactor. *Int J Hydrogen Energy* **22**, 521–524.
- Markov, S., Weaver, P. and Seibert, M. (1997b) Spiral tubular bioreactors for hydrogen production by photosynthetic microorganisms—design and operation. *Appl Biochem Biotechnol* **63–65**, 577–584.
- Merzlyak, M. and Naqvi, K. (2000) On recording the true absorption spectrum and scattering spectrum of a turbid sample: application to cell suspensions of cyanobacterium *Anabaena variabilis*. *J Photochem Photobiol B* **58**, 123–129.
- Pinto, F., Troshina, O. and Lindblad, P. (2002) A brief look at three decades of research on cyanobacterial hydrogen evolution. *Int J Hydrogen Energy* **27**, 1209–1215.
- Prince, R.C. and Ksheshgi, H.S. (2005) The photobiological production of hydrogen: potential efficiency and effectiveness as a renewable fuel. *Crit Rev Microbiol* **31**, 19–31.
- Shah, V., Garg, N. and Madamwar, D. (2001) Ultrastructure of the fresh water cyanobacterium *Anabaena variabilis* SPU 003 and its application for oxygen-free hydrogen production. *FEMS Microbiol Lett* **194**, 71–75.
- Smith, L., McCarthy, P. and Kitanidis, P. (1998) Spreadsheet method for evaluation of biochemical reaction rate coefficients and their uncertainties by weighted nonlinear least-squares analysis of the integrated monod equation. *Appl Environ Microbiol* **64**, 2044–2050.



- Sveshnikov, D., Sveshnikova, N., Rao, K. and Hall, D. (1997) Hydrogen metabolism of mutant forms of *Anabaena variabilis* in continuous cultures and under nutritional stress. *FEMS Microbiol Lett* **147**, 297–301.
- Tsygankov, A., Serebryakova, L., Rao, K. and Hall, D. (1998) Acetylene reduction and hydrogen photoproduction by wild-type and mutant strains of *Anabaena* at different CO<sub>2</sub> and O<sub>2</sub> concentrations. *FEMS Microbiol Lett* **167**, 13–17.
- Tsygankov, A., Bordin, V., Rao, K. and Hall, D. (1999) H<sub>2</sub> photoproduction by batch culture of *Anabaena variabilis* ATCC 29413 and its mutant PK84 in a photobioreactor. *Biotechnol Bioeng* **64**, 709–715.
- Tsygankov, A., Fedorov, A., Kosourov, S. and Rao, K. (2002) Hydrogen production by cyanobacteria in an automated outdoor photobioreactor under aerobic conditions. *Biotechnol Bioeng* **80**, 777–715.
- 22 Yoon, J., Sim, S., Kim, M. and Park, T. (2002) High cell density culture of *Anabaena variabilis* using repeated injections of carbon dioxide for the production of hydrogen. *Int J Hydrogen Energy* **27**, 1265–1270.
- Yoon, J., Shin, J., Kim, M., Sim, S. and Park, T. (2006) Evaluation of conversion efficiency of light to hydrogen energy by *Anabaena variabilis*. *Int J Hydrogen Energy* **31**, 721–727.

## Author Query Form

Journal: JAM

Article: 3559

Dear Author,

During the copy-editing of your paper, the following queries arose. Please respond to these by marking up your proofs with the necessary changes/additions. Please write your answers on the query sheet if there is insufficient space on the page proofs. Please write clearly and follow the conventions shown on the attached corrections sheet. If returning the proof by fax do not write too close to the paper's edge. Please remember that illegible mark-ups may delay publication.

Many thanks for your assistance.

Query reference	Query	Remarks
1	Au: Please approve or amend the suggested short title.	
2	Au: Please check author affiliations and correspondence field.	
3	Au: Please supply upto six keywords for indexing.	
4	Au: Please check the ref. citation here.	
5	Au: Bordin, Tsygankov, Rao and Hall, 2000 has been changed to Borodin <i>et al.</i> 2000 so that this citation matches the list	
6	Au: Madamwar et al., 2002 has not been included in the list, please supply publication details.	
7	Au: Markov, Lichtl, Rao and Hall (1993) has been changed to Markav <i>et al.</i> (1993) so that this citation matches the list	
8	Au: Please provide city and state if applicable.	
9	Au: Please provide city and state name here.	
10	Au: Please provide state name here.	
11	Au: Please provide city and state here.	
12	Au: Please provide city and state here.	
13	Au: Please give manufacturer information: town, state (if USA) and country.	
14	Au: Please provide city and state here.	
15	Au: Please give manufacturer information: town, state (if USA) and country.	
16	Au: Please provide city and state here.	
17	Au: Markav, Thomas, Bazin and Hall, 1997a has been changed to Markov <i>et al.</i> 1997a so that this citation matches the list	
18	Au: Please provide publisher and location if applicable.	

19	Au: Please update the ref. Berberoğlu et al. (2007) with vol. no. and page range if applicable.	
20	Au: Please provide the location for the book.	
21	Au: Please check this website address and confirm that it is correct. And also check the details of the reference.	
22	Au: Please check the page range here.	
23	Au: Makrov, Bazine and Hall, 1995 has been changed to Markov <i>et al.</i> 1995 so that this citation matches the list	

# MARKED PROOF

## Please correct and return this set

Please use the proof correction marks shown below for all alterations and corrections. If you wish to return your proof by fax you should ensure that all amendments are written clearly in dark ink and are made well within the page margins.

<i>Instruction to printer</i>	<i>Textual mark</i>	<i>Marginal mark</i>
Leave unchanged	... under matter to remain	Ⓟ
Insert in text the matter indicated in the margin	∧	New matter followed by ∧ or ∧ <sup>Ⓢ</sup>
Delete	/ through single character, rule or underline or ┌───┐ through all characters to be deleted	Ⓞ or Ⓞ <sup>Ⓢ</sup>
Substitute character or substitute part of one or more word(s)	/ through letter or ┌───┐ through characters	new character / or new characters /
Change to italics	— under matter to be changed	↙
Change to capitals	≡ under matter to be changed	≡
Change to small capitals	≡ under matter to be changed	≡
Change to bold type	~ under matter to be changed	~
Change to bold italic	≈ under matter to be changed	≈
Change to lower case	Encircle matter to be changed	≡
Change italic to upright type	(As above)	⊕
Change bold to non-bold type	(As above)	⊖
Insert 'superior' character	/ through character or ∧ where required	Υ or Υ under character e.g. Υ or Υ
Insert 'inferior' character	(As above)	∧ over character e.g. ∧
Insert full stop	(As above)	⊙
Insert comma	(As above)	,
Insert single quotation marks	(As above)	ʹ or ʸ and/or ʹ or ʸ
Insert double quotation marks	(As above)	“ or ” and/or ” or ”
Insert hyphen	(As above)	⊥
Start new paragraph	┌	┌
No new paragraph	┐	┐
Transpose	└┐	└┐
Close up	linking ○ characters	○
Insert or substitute space between characters or words	/ through character or ∧ where required	Υ
Reduce space between characters or words		↑